JOSEPH J. SUTER

ADVANCES IN THE DEVELOPMENT OF PIEZOELECTRIC QUARTZ-CRYSTAL OSCILLATORS, HYDROGEN MASERS, AND SUPERCONDUCTING FREQUENCY STANDARDS

Piezoelectric quartz-crystal oscillators, hydrogen masers, and superconducting oscillators represent classes of frequency standards that are expected to form the foundation for future systems requiring precision time and frequency sources. This article discusses advances made in the radiation-hardening of piezoelectric quartz oscillators, the future development of hydrogen masers for improved short- and long-term stabilities, and the planned development of a 10-GHz low-phase-noise oscillator using superconductors with high temperatures of transition.

INTRODUCTION

In the past, APL's Space Department has developed a series of high-quality frequency standards, including space-qualified piezoelectric quartz-crystal oscillators and hydrogen masers for terrestrial applications. The continuous demand for increased performance from these frequency standards provided the impetus for the initiation of an oscillator and hydrogen-maser improvement program. Since the radiation susceptibility of piezoelectric quartz-crystal oscillators has been recognized as a major area for improvement of spaceflight oscillators, a comprehensive study of the effects of space radiation on quartz-crystal oscillators was begun. Those studies, which employ simulation tests of low-earth-orbit radiation environments using a proton cyclotron, will provide the foundation on which the future development of radiation-hardened oscillators will be based.

Hydrogen masers, which represent the most stable oscillators of all existing atomic frequency standards, require further improvement of their frequency stability in order to meet future requirements for radio astronomy, plate tectonics and seismology, worldwide time synchronization, deep-space satellite missions, and experiments that will verify the fundamental concepts of relativity. APL's maser-improvement program focuses on reducing the thermal noise and noise from other sources in the maser, on improving the maser's long-term stability by using improved magnetic- state-selection methods, on increasing the confinement time of hydrogen atoms, and on gaining a better understanding of the relaxation processes in the hydrogen maser.

Future requirements for airborne radar demand the development of a small, acceleration- and vibration-insensitive, low-power-consumption 10-GHz oscillator that must meet stringent phase-noise specifications not met by existing technology. APL will develop a superconducting oscillator using the latest advances in the field of high-temperature ceramic superconductors, whose high temperatures of transition have made their use feasible for precision oscillators.

Although this article will discuss three major areas of research in the field of time and frequency (that is, piezoelectric quartz oscillators, hydrogen masers, and superconducting oscillators), the Space Department's Time and Frequency Systems Section has also developed satellite transmitters, laser retroreflector arrays for satellite navigation, and frequency multipliers and clock systems.[1] Furthermore, the Time and Frequency Standards Laboratory, as a member of the Bureau Internationale des Poids et Measures network, contributes to the definition of the standard second.

PIEZOELECTRIC QUARTZ-CRYSTAL OSCILLATORS

The radiation susceptibility of quartz resonators is an important parameter defining the performance of an ultrastable spacecraft oscillator. Many studies have attempted to establish a relationship between some basic properties of quartz material and the radiation response of resonators made from quartz.[2] Most of these studies involved radiation at high doses and at high dose rates using gamma rays or electrons.

Interest in the radiation sensitivity of quartz-crystal resonators stems from a long-term involvement with the design and development of spaceflight-qualified oscillators. In 1959, APL developed its first-generation spaceflight oscillator, which had a frequency stability of several parts in 10^9, for the Transit 1A program. Since then, ultrastable space oscillators have undergone many design changes that have incorporated new concepts and technologies. Oscillators produced from the current design exhibit stabilities of parts in 10^{13}. In the last 25 years, APL has designed, fabricated, and tested over 200 spaceflight-qualified oscillators for a variety of sponsors and applications.

Oscillators developed at APL have been used in many different satellites whose orbits exposed them to a wide range of space-radiation environments. To meet the various mission requirements, radiation-hardened oscillators were developed to meet proton radiation specifications in both high- and low-dose-rate environments. For missions with stringent radiation specifications, extensive and time-consuming screening of the resonators was required to meet operational requirements, primarily because of a lack of understanding of the radiation susceptibility mechanisms. This led APL to initiate preliminary studies of low-level radiation susceptibility. The results of those studies will be discussed in some detail, but first some basic properties of quartz crystal resonators will be reviewed.

The piezoelectric effect was discovered by Pierre and Jacques Curie in 1880 in their studies of the physical properties of natural quartz and rochelle salt. The publication by Voight (in 1910) of the *Lehrbuch der Kristallphysik* initiated systematic theoretical and experimental studies of piezoelectricity.[3]

The only form of synthetic quartz used for precision resonators is alpha quartz, which belongs to the trigonal crystal class with point group 32. The oxygen ions in silica quartz (SiO_2) form a tetrahedral bond with the silicon ions, resulting in a structure with unit cell dimensions of 0.491 nm (a_0) and 0.540 nm (c_0) at 300 K (Fig. 1). Investigations have shown that the unit cell dimensions of quartz are temperature-dependent, resulting in the variations of the resonance frequency of crystal resonators as a function of temperature.[4] Above 573°C, alpha quartz undergoes a phase transformation to beta quartz, with a hexagonal crystal structure. Beta quartz, when cooled below 573°, will transform to alpha quartz, which will be electrically twinned in the process; this very undesirable characteristic prohibits this quartz from being used in precision quartz resonators. Synthetic quartz is grown using a hydrothermal process in which a natural quartz nutrient is dissolved in sodium hydroxide, then evaporated and condensed onto a seed. Additions of lithium to the solute have shown that greatly improved microwave resonator Q can be achieved without the presence of lithium ions in the final quartz bars.[5] Apparently, the lithium prevents formation of OH^-, H_2O, or other impurities in the quartz, resulting in a high-purity quartz bar. This major technologic development in the quartz growth process has yielded piezoelectric quartz resonators with a Q of 2.5×10^6 at room temperature.

The piezoelectric effect in quartz crystals is described by two equations. The direct piezoelectric effect describes the relation between the polarization P of a crystal and external stresses σ, and may be expressed in tensor notation as[6]

$$P_i = d_{ijk}\sigma_{jk} + \epsilon_{ij}E_j \ , \qquad (1)$$

where P_i is the electric polarization vector, d_{ijk} is the third-rank piezoelectric strain tensor, σ_{jk} is the second-rank stress tensor, ϵ_{ij} is the second-rank permittivity tensor, and E_j is the electric field vector. The constitutive equation for the converse piezoelectric effect is

$$\sigma_{ij} = c_{ijkl}\, u_{kl} - e_{kij}E_k \ , \qquad (2)$$

where c_{ijkl} is the fourth-rank elastic stiffness tensor, u_{kl} is the second-rank strain tensor, and e_{kij} is the third-rank piezoelectric stress tensor. (Both Eqs. 1 and 2 adopt the Einstein summation convention, i.e., summation over repeated indexes.)

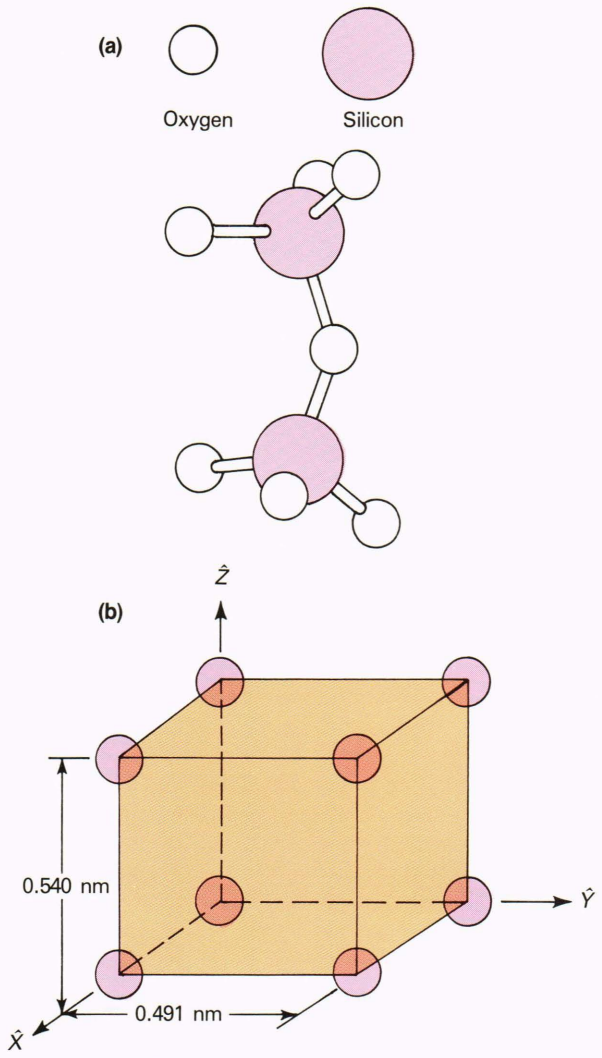

Figure 1—(a) SiO_2 bonding in alpha quartz, and (b) its unit cell.

Equations 1 and 2 are valid only for linear effects, that is, when a linear relationship between stress and strain (and also between electric polarization and stress) exists. In reality, the physical behavior of a piezoelectric crystal departs from this linear model; therefore, one must use nonlinear theory to describe the physical characteristics of a quartz crystal. Ionizing radiation incident on a quartz crystal is one cause of the departure of the crystalline material from linear behavior.

Quartz-crystal resonators are manufactured by Bragg X-ray diffraction orientation of the quartz-crystal blank,

polishing, and then mounting the crystal blank. For quartz-crystal resonators with adhered electrodes, the most widely adopted electrode configuration is central circular plating, as shown in Fig. 2a.[7] Electrodeless resonators consist of a piezoelectric-crystal blank mounted between two gold-plated quartz sections (Fig. 2b). The advantages of this design are that the electrodes do not mechanically load the active quartz plate and that no impurities can be trapped between the electrodes and quartz crystal.

To make use of the high Q, resonators are integrated in an oscillator circuit. All quartz-crystal oscillators consist of two parts: an amplifier and a feedback loop that provides feedback at the resonant frequency of the crystal. Furthermore, the quartz-crystal resonator and associated electronics are placed in an oven so that the resonator can operate at the crystal's turnover temperature (the temperature at which the frequency-versus-temperature curve of a piezoelectric crystal is a minimum).

RADIATION-SUSCEPTIBILITY STUDIES OF QUARTZ-CRYSTAL RESONATORS

The system performance of satellites requires quartz-crystal resonators with superior stability (less than 5×10^{-13} with a 1000-s integration time). Those crystal resonators must therefore be insensitive to magnetic fields, vibration, and ionizing radiation, which has been recognized as a major source affecting the quartz-crystal resonator's frequency stability. The apparent susceptibility of quartz-crystal resonators to the electron and proton radiation encountered by satellites orbiting the earth manifests itself as frequency shifts in the crystals. Early studies indicated that aluminum defect centers within the quartz crystal are responsible for frequency shifts in quartz-crystal resonators exposed to high levels (approximately 100 rad) of radiation.[2] Studies conducted at APL of the sensitivity of quartz crystals to lower dose levels (less than 10 rad), like those encountered in low earth orbits, did not reveal any correlation between aluminum impurity content and radiation sensitivity.[8] A series of experiments reported below shows a correlation between the configuration of the electrodes in crystal resonators (crystals with adhered electrodes and electrodeless crystals) and their sensitivity to low doses of ionizing radiation.

The radiation encountered in space by a satellite consists primarily of charged particles in the Van Allen belts. Those belts contain electrons and protons that interact with the quartz-crystal resonator and induce frequency shifts. Figure 3 shows the accumulated doses of electron and proton radiation as a function of shielding thickness for a 1400-km low earth orbit.[9] It is apparent that for shielding thicknesses in excess of 3 gm/cm^2 of aluminum, protons are the most significant contributor to the radiation incident on the spacecraft. The magnitude of the proton radiation received during each orbit cannot always be reduced by radiation shields. As shown in Fig. 3, no significant reduction in proton radiation occurs for single-shield thicknesses in excess of 6 gm/ cm^2. Therefore, APL has been investigating the basic radiation-sensitivity mechanism of quartz-crystal resonators, with the objective of eliminating the need for heavy radiation shields in spaceflight oscillators.

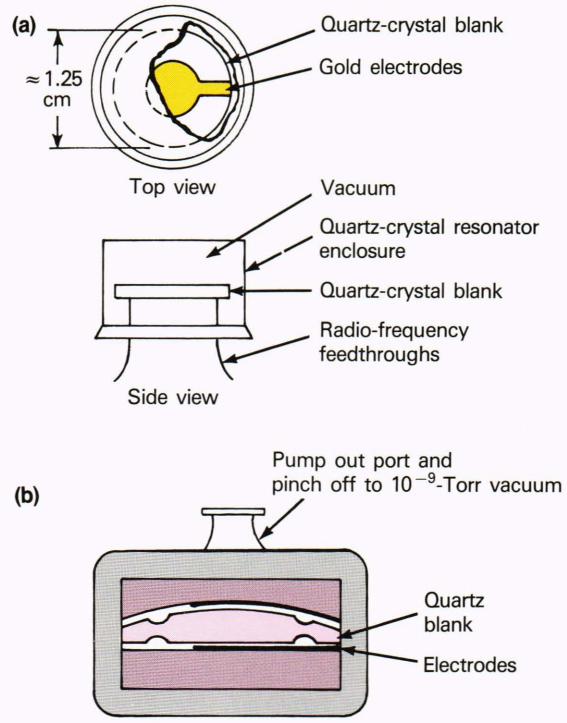

Figure 2—Simplified diagrams of quartz-crystal resonators; (a) a quartz resonator with adhered electrodes, and (b) an electrodeless quartz crystal.[7]

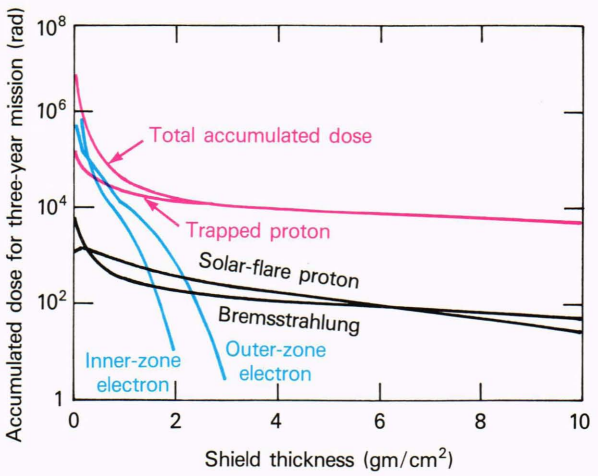

Figure 3—Expected total accumulated dose for the three-year NASA TOPEX mission.[9]

To simulate the proton-radiation environment encountered by quartz crystals in space, one must model the energy spectrum of the proton radiation. A quantitative study of a low earth orbit led to a proton-radiation model and the development of tests to simulate proton radiation using the Harvard University cyclotron.[10]

A range modulator was designed for a specific curve of dose versus penetration depth in materials, so that

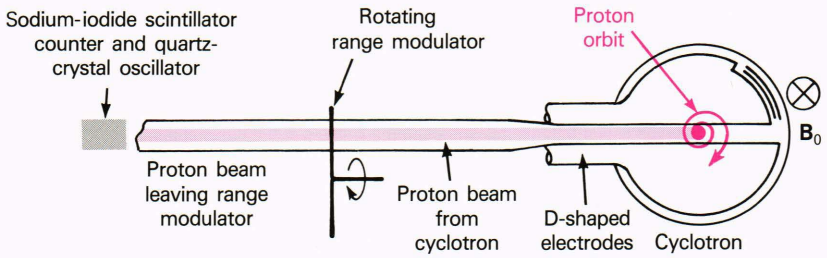

Figure 4—Simplified diagram of the Harvard University cyclotron range modulator, sodium-iodide scintillator counter, and quartz-crystal oscillator (not to scale) (©1987, IEEE).[10]

the protons could be deposited at specific depths. Such a range-modulator system (similar to the one used for the present study) is currently in use at Harvard University to treat cancer patients needing proton-beam radiation therapy.[11] As shown in Fig. 4, a large wheel is rotated across the proton beam with its axis parallel to, but not concentric with, the beam. The thickness of the wheel is not uniform, but is varied in small steps; the edge of each step follows a radius of the wheel. Protons following a particular ray of the beam encounter varying amounts of attenuation as the wheel is turned, so that the transmitted energy along that ray varies stepwise with time. The included angle for each step determines the fraction of time that each value of proton energy is present, and the time-averaged energy spectrum is then a composite determined by the geometry of the steps in the wheel. The difficulty in this case was to design the wheel geometry so that the average spectrum approximated the spectrum expected at the quartz-crystal resonator blanks in the orbiting spacecraft.

The low-earth-orbit radiation spectrum selected for the studies consisted of protons with a kinetic energy range of 10 to 120 MeV, selected on the basis of previous studies that showed that these proton energies produced the greatest frequency shifts in quartz-crystal resonators.[8] Figure 5 shows the differential proton-energy spectrum encountered in this low earth orbit after a degradation through 4 mm of spacecraft aluminum shielding.

The range modulator consisted of a set of acrylic blades of varying thickness (Fig. 6). The thickness of each acrylic blade was designed so the transmitted flux matches the required low-earth-orbit spectrum. If E_n is the calculated proton energy in MeV after degrading through n layers of acrylic, and ϕ_n is the relative transmitted flux through n layers of thickness d_n, then the thickness of the nth acrylic blade is

$$d_n = \left(\frac{dn_{\mathrm{pr}}}{dE}\right)_{E_n} \phi_n^{-1}\, \Delta E_n \ , \qquad (3)$$

where $(dn_{\mathrm{pr}}/dE)_{E_n}$ is the proton flux at an energy E_n in the space environment.[10] The energy difference of the protons after passing through alternate acrylic blades is

$$\Delta E_n = \frac{E_{(n+1)} - E_{(n-1)}}{2} \ . \qquad (4)$$

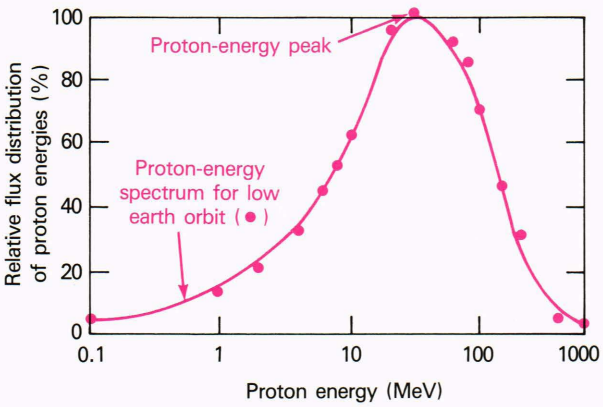

Figure 5—Proton energy distribution for a low earth orbit, as degraded by 4 mm of aluminum (©1987, IEEE).[10]

Equation 4 neglects mixing between adjacent energy bins, but the use of 6.4-mm stock acrylic ensured that mixing between bins did not distort the overall spectrum.

In the first series of tests, the AT-cut quartz-crystal resonators (AT-cut resonators are the most popular class of crystals used for spaceflight oscillators) with adhered electrodes and the electrodeless-design crystal resonators were allowed to accumulate 1 and 3 rad at a rate of 0.1 rad/min. That dose rate represents the dose rates encountered in typical low earth orbits.[12] Figure 7 shows the frequency shifts as a function of accumulated doses for the AT-cut crystal resonators. It is apparent that the electrodeless crystal resonator's frequency shift is significantly lower than the AT-cut resonator with the adhered electrodes. This is presently attributed to the electrodeless configuration of these resonators and the absence of impurities between the electrodes and quartz-crystal blank. As mentioned previously, it was generally believed that the radiation sensitivity of quartz-crystal resonators is correlated to the concentration of aluminum defect centers. To investigate the existence of any such correlation, the aluminum-defect-center concentration of the quartz crystals was measured using electron-spin-resonance techniques. Those studies revealed that the quartz crystal with the lowest frequency shift (BVA-AT) had the highest aluminum-defect-center concentration (greater than 19 ppm). That finding shows that a correlation probably does not exist between low radiation sensitivity and low aluminum-defect-center concentration.

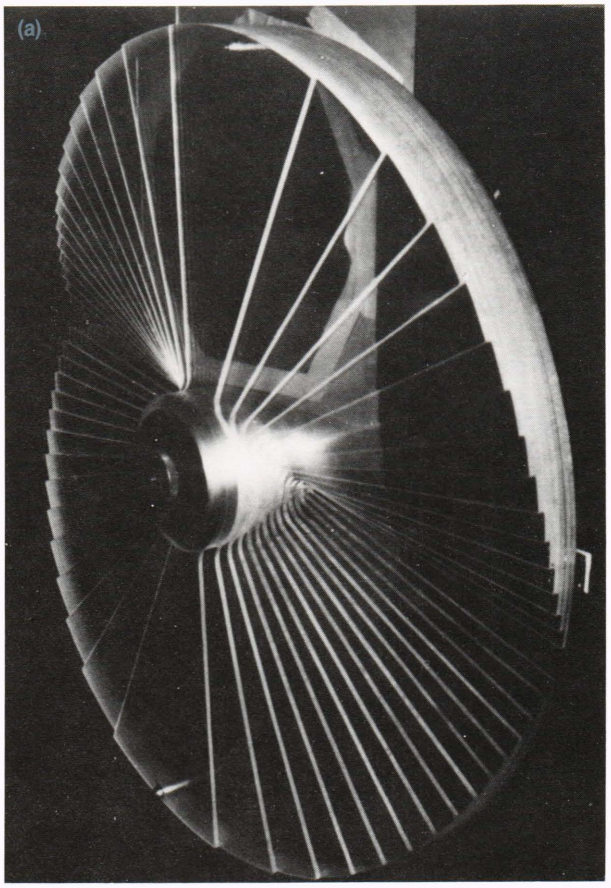

(b)

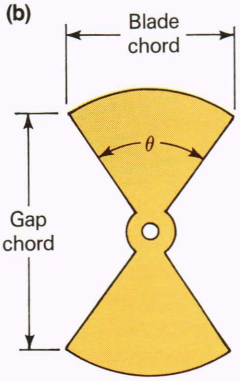

Layer	Blade angle, θ (deg)	Blade chord (cm)	Gap chord (cm)
1	175.59	82.50	3.18
2	170.99	82.30	6.48
3	166.00	82.19	10.06
4	160.52	81.36	13.97
5	154.56	80.52	18.20
6	148.15	79.38	22.66
7	140.98	77.80	27.56
8	133.07	75.72	32.87
9	124.16	72.95	38.66
10	114.27	69.34	44.81
11	103.32	64.74	51.21
12	90.77	58.75	57.99
13	75.86	50.75	65.13
14	57.10	39.45	72.52
15	29.96	21.34	79.56

Figure 6—(a) Photograph of the proton modulator wheel, and (b) mechanical layout and parameters of the proton range modulator wheel. (©1987, IEEE).[10]

The initial results show that electrodeless resonators (BVA-AT) have a lower radiation susceptibility than AT resonators with adhered electrodes, and show the need for further investigations of the materials and physical properties (piezoelectric effect) of alpha quartz-crystal resonators in the development of optimum radiation-hardened spaceflight oscillators.

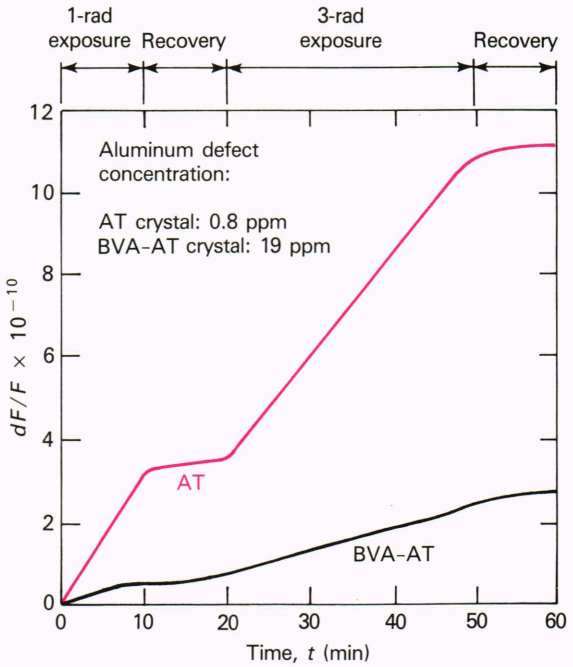

Figure 7—Frequency shifts in AT and electrodeless BVA-AT quartz-crystal resonators as a function of accumulated dose for a 0.1-rad/min simulated low earth orbit proton radiation environment.

HYDROGEN MASERS

Many applications require and benefit from the performance of the hydrogen maser. NASA's very-long-baseline interferometry project uses hydrogen masers for measurements of tectonic-plate movements, measurements of global distances, and experiments to verify fundamental concepts of relativity. The radio-astronomy community uses hydrogen masers as stable local oscillators in receivers.[13]

The 14 hydrogen masers developed by APL for NASA are all active masers.[14] This means that the maser can be considered an oscillator that receives its energy from an atomic transition in the 2 $S_{1/2}$ ground state of the hydrogen atom. The hydrogen-maser signal at a wavelength of 21 cm (a frequency of 1.4 GHz) is generated by the transition between the $F = 1$, $m_F = 0$ and the $F = 0$, $m_F = 0$ hyperfine states. The quantum number m_F identifies a Zeeman sublevel.

In practice, an atomic hydrogen beam emerges from an RF dissociator, after which a magnetic- state selector focuses hydrogen atoms in the $F = 1$, $m_F = 0$ and $F = 0$, $m_F = 0$ quantum states onto a Teflon-coated quartz storage bulb (Fig. 8). The bulb is located symmetrically within a microwave cavity that is resonant at 1.4 GHz in the transverse electric mode (TE_{011}). The quartz storage bulb is coated with Teflon to minimize atomic perturbations caused by wall collisions and to increase the storage time of the hydrogen atoms within the microwave cavity. The frequency stability and accuracy of the hydrogen maser are credited largely to this relatively long storage time (approximately 1 s). By ap-

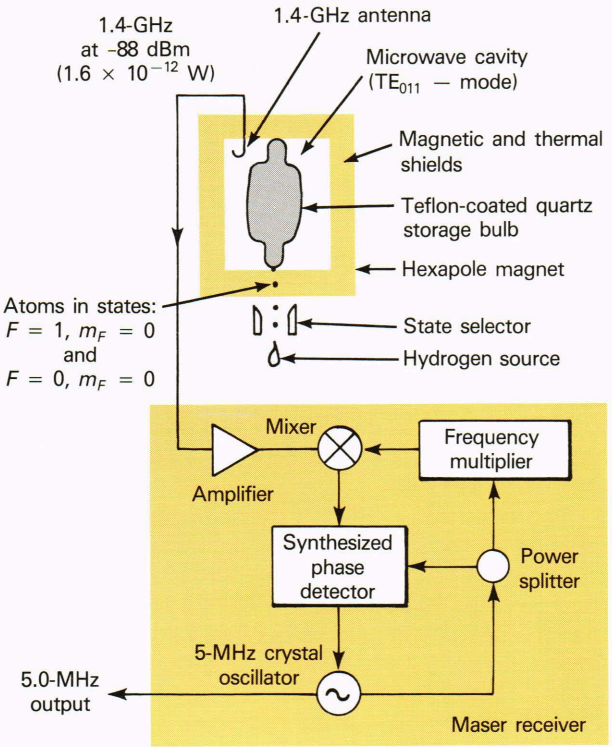

Figure 8—Simplified diagram of the hydrogen maser.

plying a small DC magnetic field (80 nT) parallel to the microwave magnetic-field component of the TE_{011} mode, the atomic transitions from the $F = 1$, $m_F = 0$ and the $F = 0$, $m_F = 0$ states can be detected using a small loop antenna. If the number of hydrogen atoms entering the quartz storage bulb exceeds 10^{12} atoms/s, and if the microwave cavity is tuned to the hyperfine transition frequency, maser oscillations occur, due to the atomic transitions, resulting in the generation of a narrowband signal (1.4 GHz ± 0.7 Hz).

The ultimate frequency stability of the hydrogen maser is directly related to the various sources perturbing the hyperfine transition's resonance line width. These sources, also known as relaxation processes, include wall relaxations, spin-exchange interactions, bulb escape, and magnetic-inhomogeneity relaxations. Each of these mechanisms can perturb the population of the energy levels and affect the coherence in the ensemble of oscillating hydrogen atoms, degrading the stability and accuracy of the maser. Noise sources such as thermal noise, white-frequency fluctuations, and random walk can degrade the frequency stability of the maser even further.

HYDROGEN-MASER RELAXATION PROCESS AND NOISE SOURCES

Controlling relaxation processes could lead to significant improvements in the frequency stability of future hydrogen masers. APL's Space Department has begun work to gain a better understanding of some of those relaxation processes and to develop practical, realizable improvements for the hydrogen maser, leading ultimately to a more stable maser. In the next section, some of the relaxation processes are discussed in some detail, together with the proposed improvements that will be incorporated in future masers.

Inhomogeneities in the applied magnetic field parallel to the microwave magnetic-field component can affect the coherence in the maser and can produce relaxations among the atom population, if it were not for the fact that that effect has been made negligible in APL's maser. By designing a set of moly-permalloy magnetic shields, a parallel DC magnetic-shielding factor greater than 100,000 has been achieved, resulting in only a very small fraction of atoms emitting microwave radiation associated with (undesirable) $\Delta m_F = \pm 1$ transitions. The DC magnetic susceptibility of the maser is now 2×10^{-15} over the $\pm 5.0 \times 10^{-5}$ T range. Therefore, the stability of the magnetic field is not a limitation on the frequency stability of the maser.

Wall relaxations in hydrogen masers originate from a perturbation of the hydrogen atom's wave function when the atoms collide with the quartz storage-bulb wall. This phenomenon may affect the population density of energy levels and the coherence in the maser. Intensive investigations have shown that coating the quartz storage bulb with FEP-120 Teflon results in one of the smallest reported wall shifts. The procedure of coating the quartz bulb with Teflon has been significantly improved. Lately, studies have concentrated on the hardness of the Teflon layer, which apparently can be increased by irradiating the Teflon-coated quartz with 1.25-MeV gamma radiation (10 krad) from a cobalt-60 source. Initial experiments with Teflon-coated quartz slides have revealed that irradiation of the Teflon surface yields stronger homopolymer bonds.

The Q_l of the atomic line of the hydrogen maser is defined as

$$Q_l \equiv \frac{f_0}{\Delta f} \approx \frac{\pi f_0}{(\gamma_b + \gamma_w + \gamma_m)} , \qquad (5)$$

where Δf is the full-width at half-amplitude of the atomic resonance line, γ_b is the bulb escape rate, γ_w is the wall relaxation constant, and γ_m is the magnetic-susceptibility relaxation constant. By reducing those relaxation constants, a narrower atomic resonance line will result. Thus, the frequency stability of the maser can be improved by reducing the relaxation rates. The impact of the relaxation processes on the frequency stability of the hydrogen maser can be characterized by the two-sample (Allan) variance in the time domain t, where t is the time during which the frequency is measured. The contributions of those noise sources bounds the Allan Variance, $\sigma(\tau)$, of the hydrogen maser in the so-called short-term ($1 < \tau < 1000$ s) and long-term ($\tau > 1000$ s) regions.

Thermal noise, σ_{th}, in a hydrogen maser is generated in the microwave cavity and receiver (Fig. 9). It has been shown that this noise can be expressed as[15]

$$\sigma_{th}(\tau) = \left[\frac{kT}{2P_0 Q_l^2 \tau}\right]^{1/2} , \qquad (6)$$

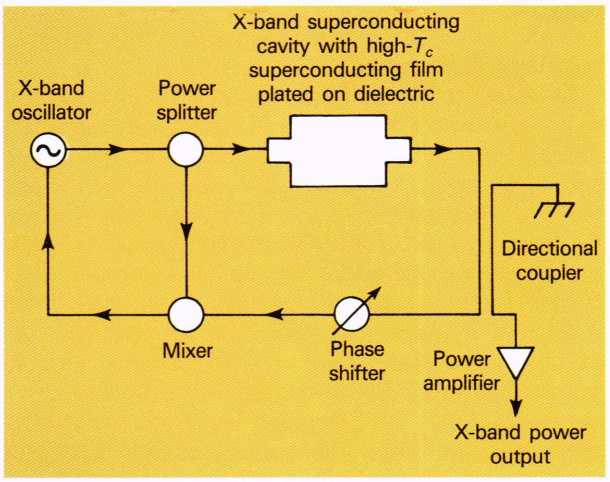

Figure 9—Simplified functional block diagram of a low-phase-noise superconducting oscillator.

where k is Boltzmann's constant, T is the temperature of the maser cavity, P_0 is the power output of the hyperfine maser transition, and Q_1 is the line Q of the atomic resonance line. The signal-to-noise ratio can be improved by increasing P_0. That requires that the state-selection process, in which an inhomogeneous magnetic field develops a force that deflects hydrogen atoms into two groups according to the direction of electron spin (parallel or antiparallel), be done more efficiently. This will be done in the next series of masers by using a hexapole-permanent-magnet state selector that focuses atoms in the $F = 1$, $m_F = 0$ and $F = 0$, $m_F = 0$ states, producing an improved population inversion in the storage bulb.[1] The signal-to-noise ratio in the maser can also be improved by decreasing the escape rate and increasing the confinement time of hydrogen atoms in the storage bulb, which, by Eq. 5, will cause the line Q to increase.

Another form of noise affecting the short-term stability of the hydrogen maser is additive phase noise, representing frequency fluctuations at the maser receiver input. This form of noise may be expressed as[16]

$$\sigma_{pn} = \left[\frac{kTFB}{4\pi^2 f_0^2 \tau^2 P}\right]^{1/2}, \tag{7}$$

where F and B are the noise figure and bandwidth of the receiver, respectively. P is the power delivered to the receiver, which is related to P_0 by

$$P = \left(\frac{\beta}{1+\beta}\right) P_0 , \tag{8}$$

where β is the coefficient of coupling for the microwave cavity. It is apparent from Eq. 7 that noise degradation of the maser's frequency stability is proportional to the square root of the receiver's noise figure and bandwidth. Therefore, by reducing those two parameters, an improvement in stability could result.

A further reduction of white-frequency noise could be accomplished by increasing P, since this quantity is related to the total power radiated by the hydrogen atoms (P_0) through Eq. 8. Furthermore, by increasing β, more power can be extracted from the maser cavity, resulting in increased frequency stability. An increase in coupling also reduces the Q of the loaded microwave cavity, since

$$Q = \frac{Q_0}{(1+\beta)} , \tag{9}$$

where Q_0 is the unloaded-cavity quality factor. Such a reduction in loaded Q could affect the long-term stability of the hydrogen maser. Therefore, a study will be conducted of the relationship between β and the maser's long-term stability.

The long-term stability of the hydrogen maser is also affected by the susceptibility of the maser's microwave cavity to temperature variations. Variations in temperature cause the microwave cavity to change its size, resulting in a degradation of the frequency stability. Several improvements have been made, which have lowered the overall temperature coefficient of the maser to 2×10^{-14} °C^{-1}. Those improvements involved the use of quartz liners and mounting fixtures with low coefficients of thermal expansion.[17] Further investigations are planned into the use of all-quartz microwave cavities in the hydrogen maser.

The physical mechanisms that define the short- and long-term stability of the hydrogen maser are complex, and important theoretical work still remains to be done. Examination of the frequency stability of the hydrogen maser as a function of fundamental parameters such as noise figure, temperature, cavity, and atomic-line Q's can establish important physical characteristics of the maser's leading to improvements in its frequency stability.

SUPERCONDUCTING OSCILLATORS

The quartz-crystal oscillators and hydrogen masers discussed so far all generate frequencies in the 5 to 100 MHz range. If particular applications require frequencies above 100 MHz, one commonly employs frequency multipliers to generate them. Unfortunately, frequency multiplication of any reference signal also magnifies noise. The increased noise level F is related to the multiplication N by

$$F = 20 \log N . \tag{10}$$

For example, multiplying a 5-MHz reference signal to 10 GHz requires a frequency multiplier with $N = 2000$, increasing F by 66 dB. Therefore, it is desirable that a frequency reference be developed to operate at the highest practical frequency, yielding maximum phase-noise performance. Several frequency standards with high fundamental frequencies have been developed.[18] The phase-noise characteristics of those devices do not meet future system specifications for radar systems. APL has

begun developing a superconducting oscillator using the latest advances in the field of high-temperature ceramic superconductors. Previous superconducting oscillators used niobium microwave cavities, which had the drawback that they needed to operate at temperatures near 1 K in order to yield cavity quality factors of order 10^9. Those oscillators could operate only for limited amounts of time in complex batch-filled liquid-helium cryostats, restricting their use to research laboratory applications. The development of superconductors such as $YBa_2Cu_3O_{7-\delta}$ with transition temperatures of approximately 90 K has made it possible to explore the applications of those ceramic materials as oscillators (see the article by Moorjani et al. elsewhere in this issue). The major advantage for using the new alkali-earth superconductors as oscillators is their high temperature of transition (greater than 90 K)—above the boiling point of nitrogen—which will reduce the complexity of cryogenic systems. The design proposed involves an X-band resonant cavity operating in a transverse electric mode, coated with a superconductor with a high temperature of transition (Fig. 9). A microwave signal generated by a high-frequency reference oscillator is incident on the microwave cavity, whose high Q ($Q \geq 10^7$) allows only the signal from the reference source to pass. That signal is then applied to a mixer, which produces an error signal that is a measure of how far the fundamental frequency of the reference oscillator is from the superconducting cavity's resonant frequency.[19] The error signal is applied to the reference oscillator, so as to change its frequency to the resonant frequency of the superconducting cavity. Such a method of controlling the frequency of the reference oscillator is expected to yield single-sideband phase noise that meets future radar requirements (Fig. 10).

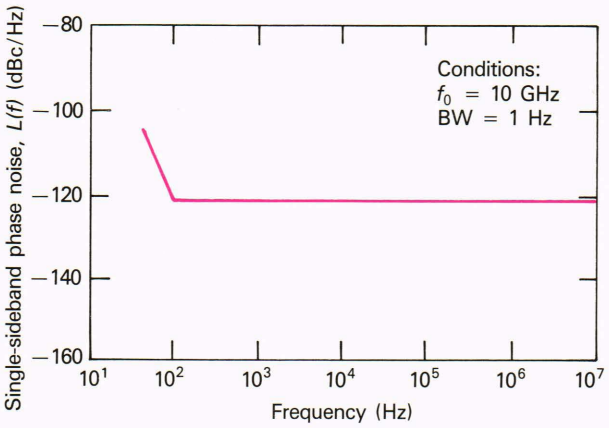

Figure 10—Projected single-sideband phase-noise performance of a 10-GHz superconducting oscillator.

REFERENCES

[1] A. G. Bates, M. T. Boies, M. C. Chiu, R. Kunski, and J. J. Suter, "Precision Time and Frequency Source and Systems Research and Development at The Johns Hopkins University Applied Physics Laboratory," in *Proc. 18th Annual Precise Time and Time Interval (PTTI) Appl. and Plan. Meeting,* Washington, pp. 55–70 (1986).

[2] L. E. Halliburton and J. J. Martin, "Properties of Piezoelectric Materials," in *Precision Frequency Control,* Vol. I, E. A. Gerber and A. Ballato, eds., Academic Press, New York, pp. 2–279 (1985).

[3] W. Voight, *Lehrbuch der Kristallphysik,* B. G. Teubner, Berlin (1910).

[4] S. Danielsson, I. Grenthe, and A. Oskarsson, "A Low Temperature Apparatus for Single Crystal Diffractometry. The Unit Cell Dimensions of Alpha-Quartz in the Temperature Range from 86–298K," *J. Appl. Crystallog.* **9**, 14–17 (1976).

[5] J. C. King, A. A. Ballman, and R. A. Laudise, "Improvement of the Mechanical Q of Quartz by the Addition of Impurities to the Growth Solution," *J. Phys. Chem. Solids* **23**, 1019–1021 (1962).

[6] J. F. Nye, *Physical Properties of Crystals,* Clarendon Press, Oxford (1985).

[7] R. J. Besson, "Résonateur à Quartz à Electrodes non Adhérentes au Cristal," *Demande de Brevet d'Invention, No: 7601035,* Institut National de la Propriété Industrielle Paris (1976).

[8] J. R. Norton, J. M. Cloeren, and J. J. Suter, "Results from Gamma Ray and Proton Beam Radiation Testing of Quartz Resonators," *IEEE Trans. Nuc. Sci.* **NS-31**, 1230–1233 (1984).

[9] P. A. March, C. M. Horton, and E. G. Stassinopoulos, *TOPEX Radiation Environment,* D-2116, Jet Propulsion Laboratory (1985).

[10] J. J. Suter, J. M. Cloeren, J. R. Norton, D. Y. Kusnierkiewicz, and A. M. Koehler, "Simulation of Low-Earth-Orbit Radiation Environments with a 5 to 120 MeV Proton Cyclotron Beam Using a Proton Beam Modulator," *IEEE Trans. Nuc. Sci.* **NS-34**, 1070–1075 (1987).

[11] L. J. Verhey, A. M. Koehler, J. C. McDonald, M. Goitein, I. C. Ma, R. J. Sneider, and M. Wagner, "The Determination of Absorbed Dose in a Proton Beam for Purposes of Charged Particle Radiation Therapy," *Radiat. Res.* **79**, 34 (1979).

[12] J. J. Suter and R. H. Maurer, "Low and Medium Dose Radiation Sensitivity of Quartz Crystal Resonators with Different Aluminum Impurity Content," *IEEE Trans. Ultrason., Ferroelectronics, and Freq. Contr.* **UFFC-34**, 667–673 (1987).

[13] J. Vanier, "The Active Hydrogen Maser: State of the Art and Forecast," *Metrologia* **18**, 173–186 (1982).

[14] L. J. Rueger, "Characteristics of the NASA Research Hydrogen Maser," *J. Inst. of Electron. Telecommun. Eng.* **27**, 493–500 (1981).

[15] R. F. C. Vessot, E. M. Mattison, R. L. Walsworth, I. F. Silvera, H. P. Godfried, and C. C. Agosta, "A Hydrogen Maser at Temperatures below 1 K," in *Proc. 14th Annual Freq. Contr. Symp.,* Philadelphia, pp. 413–418 (1986).

[16] E. M. Mattison, R. F. C. Vessot, and S. Wei, "Single-State Selection System for Hydrogen Masers," in *Proc. 14th Annual Freq. Contr. Symp.,* Philadelphia, pp. 422–427 (1986).

[17] L. J. Rueger and M. C. Chiu, "Development of Precision Time and Frequency Systems and Devices at APL," *Johns Hopkins APL Tech. Dig.* **6**, 75–84 (1985).

[18] H. Helwig, "Microwave Frequency and Time Standards," in *Precision Frequency Control,* Vol. II, E. A. Gerber and A. Ballatto, eds., Academic Press, New York, pp. 114–175 (1985).

[19] J. J. Suter and A. G. Bates, "High T_c Superconducting Stable Oscillator," patent under disclosure.

ACKNOWLEDGMENTS—The author gratefully acknowledges the contributions of A. G. Bates and L. J. Rueger. The technical contributions of J. M. Cloeren, J. R. Norton, C. R. Moore, M. T. Boies, R. J. Costlow, and M. C. Chiu are acknowledged. The support and efforts of L. E. Stillman, P. J. Underwood, J. L. Wilcox, and M. A. Restivo are also acknowledged. The financial support of the Jet Propulsion Laboratory of the California Institute of Technology, NASA Goddard Space Flight Center, the Naval Research Laboratory, and the Department of Defense is gratefully acknowledged. The author expresses his gratitude to the Independent Research and Development Program of APL and to The Johns Hopkins University Center for Nondestructive Evaluation for supporting the work on the radiation susceptibility of quartz-crystal resonators and superconductors.

THE AUTHOR

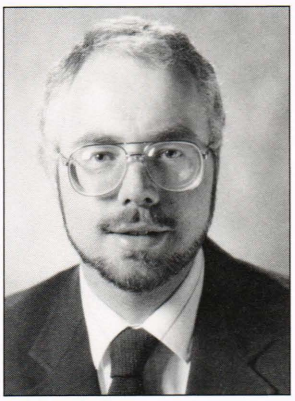

JOSEPH J. SUTER received a B.S. degree in physics in 1977 from the Free University in Amsterdam, The Netherlands, and an M.S. degree in physics from Michigan State University in 1980. From 1980 to 1982, he was a graduate research assistant at the Laboratory for Plasma and Fusion Energy Studies at the University of Maryland, where in 1982 he was awarded an M.S. degree in electrical engineering. In 1988, he received a Ph.D. degree in materials science and engineering from The Johns Hopkins University on the basis of his research on the radiation susceptibility of alpha quartz-crystal resonators. Since joining APL in 1983, Dr. Suter has been involved in the development of radiation-hardened oscillators, an improvement program for the hydrogen maser, and the development of superconducting oscillators. He is a member of the Space Department's Communications, RF, and Optical Systems Group.